



## Osthole decreases tau protein phosphorylation via PI3K/AKT/GSK-3 $\beta$ signaling pathway in Alzheimer's disease



Yingjia Yao<sup>a,1</sup>, Yameng Wang<sup>a,1</sup>, Liang Kong<sup>a</sup>, Yuqing Chen<sup>b</sup>, Jingxian Yang<sup>a,\*</sup>

<sup>a</sup> Liaoning University of Traditional Chinese Medicine, Dalian 116600, China

<sup>b</sup> Dalian University of Technology, Dalian 116024, China

### ARTICLE INFO

#### Keywords:

Alzheimer's disease  
Phosphorylated tau protein  
Apoptosis  
PI3K  
Osthole

### ABSTRACT

**Aim:** Alzheimer's disease (AD), a neurodegenerative disease, was characterized by the loss of memory and progressive cognitive deterioration. Up to now, there has no effective drugs to cure or delay the state of illness. Increasing evidence indicates that hyperphosphorylated tau protein plays a pivotal role in the occurrence and development of AD. Therefore, in present study, we aim to investigate whether osthole (OST) could decrease hyperphosphorylated tau protein in AD and the underlying mechanism.

**Main methods:** The ability of learning and memory was detected by Morris Water Maze. The pathological changes were detected by H&E staining. The percentage of cells apoptosis was detected by TUNEL assay *in vivo* and Flow Cytometry *in vitro*. The expressions of tau protein and related proteins in PI3K/Akt/GSK-3 $\beta$  signaling pathway were detected by Western Blot.

**Key findings:** We found that OST could significantly improve learning and memory dysfunction, ameliorate the histology structure of damaged neural cells in hippocampal area. Moreover, we also found that OST could decrease tau protein phosphorylation as well as inhibit cells apoptosis. To explore the underlying mechanism, we used LY294002 to block PI3K/Akt/GSK-3 $\beta$  signaling pathway, the results from Western blot showed that the expression of related proteins in PI3K signaling pathway were decreased with LY294002 treated.

**Significance:** Taken together, the results indicated that OST could decrease phosphorylated tau levels via activation of PI3K/Akt/GSK-3 $\beta$  signaling pathway. Thus, this study demonstrated that OST might be a potential candidate for the treatment of AD.

### 1. Introduction

Alzheimer's disease (AD), an age-related, is the most neurodegenerative disorder leading to progressive cognitive impairment. The characteristic features of AD neuropathology include  $\beta$ -amyloid plaques (A $\beta$ ), neurofibrillary tangle (NFTs), and neuronal loss in the brain [1]. AD is generally known to be correlated with accumulation of A $\beta$  which is produced from amyloid precursor protein (APP) [2]. A great number of evidences also indicate that tau protein has shown to be most closely related to the clinical manifestations of AD [3,4]. Tau, a family of neuronal proteins is the major microtubule stability associated protein of the cells. In normal human brain, it has 2–3 mol of phosphate per mole of the protein, but, in pathological conditions, it was at least 3–4-fold hyperphosphorylated and aggregated into neurofibrillary tangles [5]. Due to abnormal phosphorylation of tau, it would directly lead to the loss of its microtubule stabilizing ability and neurite degeneration.

Furthermore, it was surprised that about 20% of all aged individuals had tau pathology, but no A $\beta$  pathology in the brain [6]. Furthermore, all almost drugs targeting in A $\beta$  had failed in the different phases of clinical trials. These results suggested that it was possible that A $\beta$ , as a monotherapy, was not an effective drug target for AD. Therefore, tau-based therapeutic approaches, such as inhibition of tau hyperphosphorylation or inhibition of aggregation of tau will play a key role in AD treatment.

The phosphoinositide 3-kinase (PI3K)/AKT signaling pathway appears to be important for AD because it promotes protein hyperphosphorylation in tau [7]. Glycogen synthase kinase-3 $\beta$  (GSK-3 $\beta$ ), an important downstream target of PI3K/AKT signaling pathway, was well known for the major roles in mediating neurogenesis [8]. Accumulate evidence showed that active GSK-3 $\beta$  would contribute to the aberrant phosphorylation of tau in neurons and aggregation of neurofibrillary tangles, eventually impairment of learning and memory [9,10].

\* Corresponding author.

E-mail address: [jingxianyang0520@163.com](mailto:jingxianyang0520@163.com) (J. Yang).

<sup>1</sup> Co-author: Yingjia Yao and Yameng Wang.

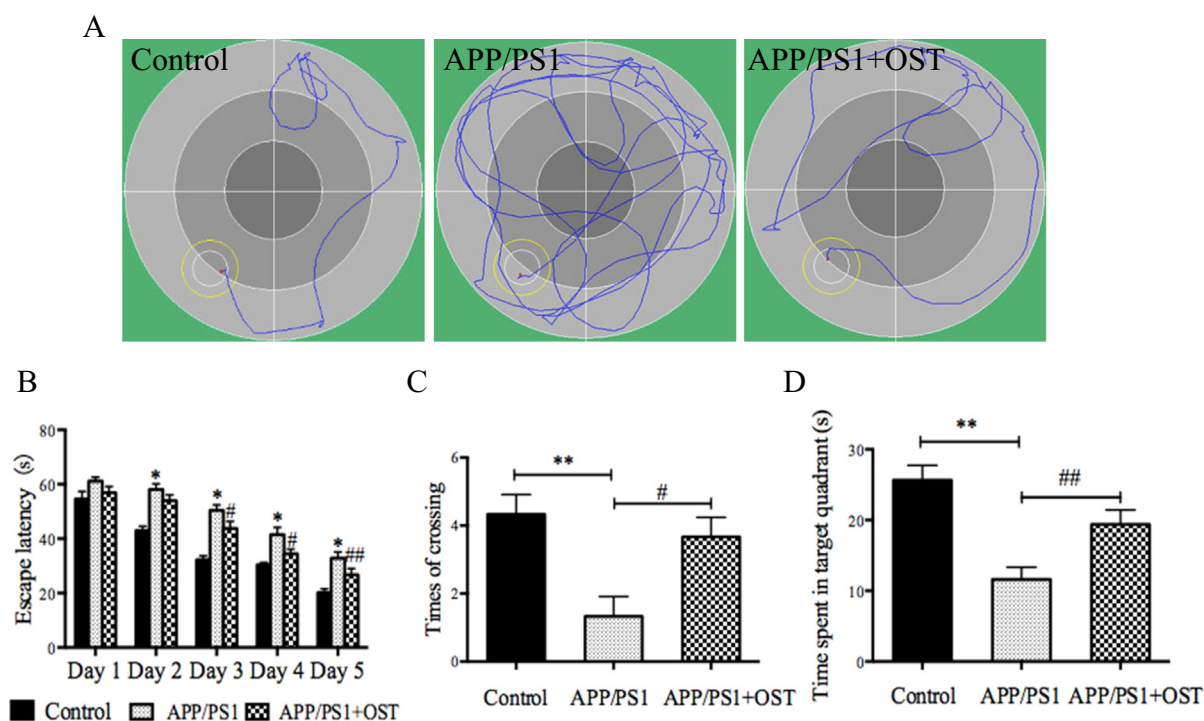


Fig. 1. The cognitive functions were detected in APP/PS1 mice.

A: The representative individual swimming paths in the Morris water maze trail on the 5th day. B: The escape latency. C: The times of crossing. D: The time spent in target quadrant. The values are expressed as the mean  $\pm$  SD. (\* $P < 0.05$ , \*\* $P < 0.01$ , # $P < 0.05$  and ## $P < 0.01$ ,  $n = 8$ , per group).

Osthole ( $C_{15}H_{16}O_3$ , 7-methoxy-8-isopentenoxycoumarin, OST) was derived from medicinal plants, including *Cnidium monnieri* (L.) Cusson. It had diverse and wide pharmacological functions, such as anti-tumor, anti-inflammatory and anti-apoptotic effects [11–13]. Our previous experimental results demonstrated that OST could protect bone marrow-derived neural stem cells against injury induced by  $H_2O_2$  through PI3K/AKT signaling pathway, it also could protect neurons synapses by the up-regulation of microRNA-9 in SH-SY5Y cells and neurons with APP overexpression [14,15]. However, OST suppressed tau protein hyperphosphorylation in SH-SY5Y cells and whether the PI3K/AKT signaling pathway was involved in this process remain unclear. In present study, we use the LY294002 to block PI3K/AKT signaling pathway to study the inhibitory effect of OST on the phosphorylation of tau protein, in order to verify that OST might become a potential application in the treatment of AD and other neurodegenerative disease.

## 2. Materials and methods

### 2.1. Preparation of drugs

OST ( $C_{15}H_{16}O_3$ , 244.39 Da), named as 7-methoxy-8-isopentenoxycoumarin, was derived from medicinal plants, such as *Cnidium monnieri* (L.) Cusson [16]. Mice in OST group were intragastric administration at a dose of 20 mg/kg twice daily for 8 weeks [17]. Cells in OST group were treated with OST for 24 h at a concentration of 100  $\mu$ M [18].

LY294002 ( $C_{19}H_{17}NO_3$ , 307.34 Da, CAS No.: 154447-36-6) is a potent and specific cell-permeable inhibitor of PI3K. It could block PI3K/AKT signaling pathway by acting on the ATP binding site of the enzyme, including p110 $\alpha$ , p110 $\delta$  and p110 $\beta$ . Cells were treated with LY294002 at a final concentration of 10  $\mu$ M [19].

### 2.2. Animal

APP/PS1 double transfected mice in a C57BL/6 background, were purchased from the Model Animal Resource Information Platform (Nanjing, China). The mice, overexpressed with mutated APP (APP<sub>swe</sub>) and mutated PS1 (PS1<sub>ΔE9</sub>) in the 6th months, can effectively simulate the pathological features of AD patients [20]. All the procedures involving mice were conducted in accordance with the Institutional Animal Care Committee of Liaoning University of Traditional Chinese Medicine. The female mice were housed 4 per cage under standard conditions (free access to food and water; 12-h light/dark cycle). APP/PS1 mice were randomly divided into two groups, and Wild-Type (WT) C57BL/6 mice at the same age were served as control group ( $n = 8$  for each group).

### 2.3. Morris water maze

After 8 weeks treatment with OST, Morris water maze was used to task to assess learning and memory performance. The details were described in our previous report [21]. In brief, mice were trained to swim to the platform in a pool for 5 consecutive days. Training was consisted of 4 times of 60 s trails per day with intervals of 30 s. Escape latency, crossed times and time spent in target quadrant were determined from an auto-video tracking record.

### 2.4. HE staining and Nissl staining

Haematoxylin and Eosin (HE) staining was used frequently in histology to examine sections of brain. Nissl staining was also revealed that the histological method for visualizing neurons in the brain. The sections were incubated with reagents according the staining assays' instructions [22,23].

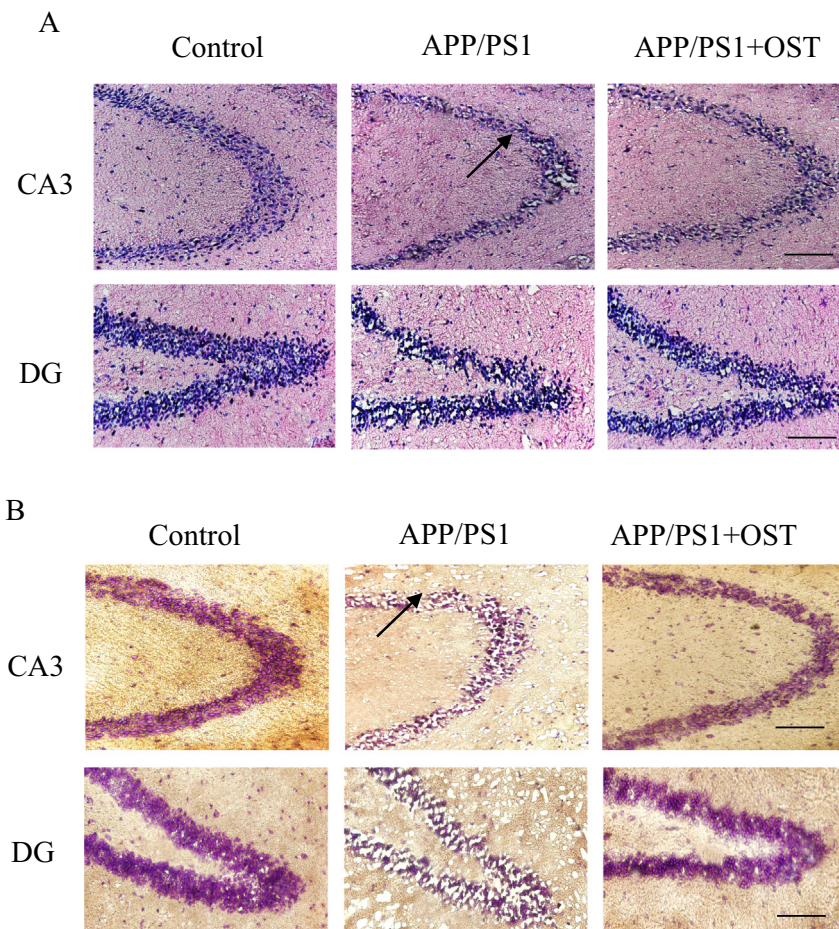


**Fig. 2.** The histological changes of brains in hippocampal areas.

A: Representative photos of H&E staining in hippocampal area. Scale bar = 100  $\mu$ m. B: Representative photos of Nissl staining in hippocampal area. Scale bar = 100  $\mu$ m. Black arrows pointed out the damaged neurons. (n = 6, per group).

### 2.5. Western blot

Total protein from cells or brain samples was extracted with protein lysis buffer, and the concentration was determined using Bradford assay. 30  $\mu$ g were added into 10% sodium dodecyl sulfate polyacrylamide gel (SDS-PAGE), then transferred onto a nitrocellulose membrane. The protein on the membranes was incubated with primary antibodies included rabbit anti-tau (1: 1000, Cat. No. bs-0419R, Bisso, China), anti-phospho-tau (Ser202, 1: 500, Cat. No. bs-11240R, Bisso, China), anti- $\beta$ -actin (1:1000, bs-0061R, Bisso, China), anti-PI3K (p110 $\alpha$  (C73F8), 1: 1000, Cat. No. 4249, CST, USA), anti-Akt (1: 500, Cat. No. 9272, CST, USA), anti-phospho-Akt (Ser473, 1: 1000, Cat. No. 4060, CST, USA), anti-phospho-GSK-3 $\beta$  (Ser9, 1:1000, Cat. No. 9323, CST, USA). Then, the membranes were washed with TBST buffer, and incubated in secondary horseradish peroxidase-conjugated anti-rabbit IgG antibody for 1 h at room temperature (RT). Finally, the membranes were colorized with a DAB kit using ImageJ software to determine protein expression levels.

### 2.6. Cell culture and transfection

Human neuroblastoma (SH-SY5Y) cells and Human embryonic kidney (HEK 293) were cultured in Dulbecco's modified Eagle's medium (DMEM) supplemented with 10% fetal bovine serum (FBS), 100 U/ml of penicillin and 100  $\mu$ g/ml streptomycin (all from Gibco, USA) at 37  $^{\circ}$ C in a 5% CO<sub>2</sub> humidification incubator. Then, the lentiviral vectors with APP-GFP and three helper plasmids, such as pLP1, pLP2 and pLP/VSV-G were fused into HEK 293 cells [24]. The virus supernatants were

collected, transfected into SH-SY5Y cells, GFP as control group. We used RT-PCR and Western blot methods to determine the expressions of APP mRNA and protein to confirm whether AD cells model was established successfully.

### 2.7. Reverse transcription-PCR (RT-PCR)

Total RNA was extracted using TRIZOL reagent (Sigma Aldrich, USA), cDNA was synthesized by using a Revert Aid First Strand cDNA Synthesis Kit (Thermo Scientific, USA). The primers for APP and  $\beta$ -actin gene are as following: APP-F, 5'-GAC TGA CCA CTC GAC CAG CAG GTT CTG-3' and APP-R, 5'-CTT GTA AGT TGG ATT CTC ATA TCC G-3';  $\beta$ -actin-F, 5'-GGG AAA TCG TGC GTG ACA T-3' and  $\beta$ -actin-R, 5'-TCA GGA GGA GCA ATG ATC TTG-3' (Invitrogen, USA). The PCR was carried out with the DreamTaq Green PCR Master Mix (Abm, China). The RT-PCR products were resolved in 3% agarose gel stained with ethidium bromide. Quantitative analysis was performed using a Gel Image System (Tanon 4100, Tanon Science & Technology, China).

### 2.8. Immunofluorescence assay

The SH-SY5Y cells were fixed with 4% paraformaldehyde for 30 min, and permeabilized with 1% Triton 100 (Sigma, USA) for 20 min, PBS washed 3 times. Then, the cells were blocked with 5% BSA for 30 min, subsequently, the primary antibody was incubated overnight (Rabbit anti-phospho-tau Ser202, 1: 100, Cat. No. bs-11240R, Bisso, China) at 4  $^{\circ}$ C. The next morning, wash twice with PBS, the cells were incubated with the secondary antibody (Goat anti-rabbit, 1: 500,

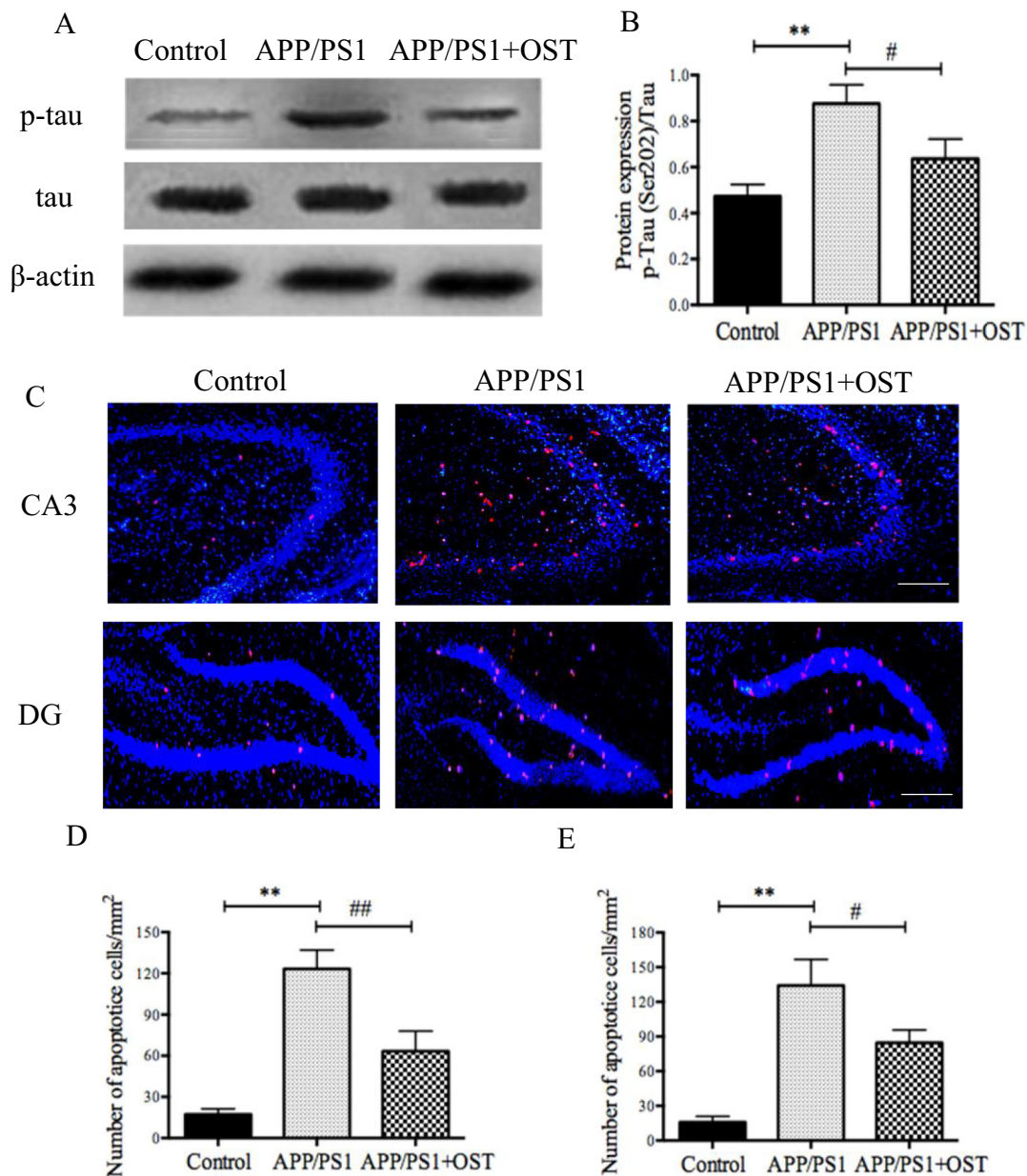


**Fig. 3.** Effects of Osthole on phosphorylation of tau protein and cells apoptosis.

A: The represent immunoblot bands of p-tau, total tau and  $\beta$ -actin protein. B: Semi-quantitative analysis of total tau protein and phosphorylated tau (Ser202) protein levels by densitometry, normalized to the level of  $\beta$ -actin ( $n = 3$ , per group). C: TUNEL/DAPI assay for detection of apoptotic cells. Scale bar = 100  $\mu$ m. D: The number of apoptotic cells in CA3 area ( $n = 6$ , per group). E: The number of apoptotic cells in DG area ( $n = 6$ , per group). The data was expressed as mean  $\pm$  SD. (\*\* $P < 0.01$ , \* $P < 0.05$  and ## $P < 0.01$ ).

Cat. No. ab6939, abcam, USA) for 1 h in the dark room at RT. Finally, DAPI was used to stained nucleus for 15 min. Fluorescence was recorded on the inverted fluorescence microscope.

## 2.9. MTT assay and LDH assay

The cells were re-seeded at a density of  $5 \times 10^3$  cells in 96-wells plate. And the cells viability and release of lactate dehydrogenase were measured by MTT assays and LDH assay, respectively, according to the manufacturer's instructions. Cells viability was expressed as a percentage of viable cells relative to GFP group using a microplate reader on the absorbance at 450 nm. The LDH levels was expressed as the percentage of LDH released into the medium relative to the total LDH activity [25].

## 2.10. TUNEL assay and Flow cytometry analysis

The brain sections were fixed with 4% paraformaldehyde for 30 min, the terminal deoxynucleotidyl transferase dUTP nick-end labeling assay (TUNEL, Transgen biotech, China) was performed according to the manufacturer's instruction [26]. The fluorescence of sections was observed under a fluorescence microscope (Nikon Eclipse E600, Japan). The cells apoptosis analyses were performed using Annexin Annexin V-FITC/propidium iodide (PI) assay (Wanlei, China) staining followed by Flow cytometric analysis.

## 2.11. Statistical analysis

All data are presented as the mean  $\pm$  standard deviation (SD) of at least three independent experiments. Statistical analysis was performed

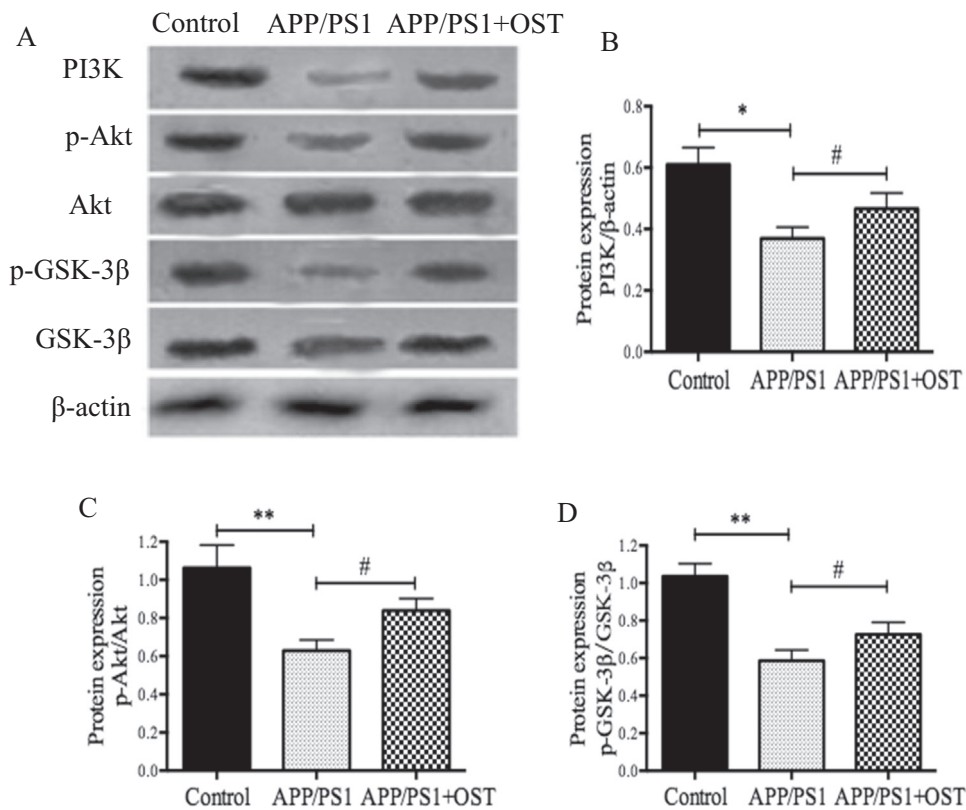


**Fig. 4.** The expression of related proteins in PI3K/Akt/GSK-3β signaling pathway.

A: The levels of proteins was detected by Western blot. B: Quantitative analysis of PI3K protein. C: The levels of p-Akt/Akt was measured. D: The levels of p-GSK-3β/GSK-3β was measured. The data was expressed as mean ± SD. (\*\* $P < 0.01$ , \* $P < 0.05$ , and # $P < 0.05$ ,  $n = 3$ , per group).

by Student's *t*-test or two-way ANOVA using GraphPad Prism 5.0 (GraphPad Prism Software, CA).  $P < 0.05$  was considered as significantly significant.

### 3. Results

#### 3.1. OST improved cognitive impairments in APP/PS1 mice

In order to investigate whether OST treatment improved the ability of learning and memory, mice were trained using the Morris water maze. The representative individual swimming paths on the 5th day was recorded by an auto-camera (Fig. 1A). In this study, as expected, in all the groups, the mice manifested shorter and shorter escape latencies at the end training trial. The differences were observed between the three groups ( $F$  value = 32.30, compared with control group, \* $P < 0.05$  in APP/PS1 group, compared to APP/PS1 group, # $P < 0.05$  and ## $P < 0.01$  in APP/PS1 + OST group, Fig. 1B). When the platform was removed, the times of crossing decreased in APP/PS1 mice ( $1.33 \pm 0.33$ ), compared to the control mice ( $4.33 \pm 0.33$ ). The times of crossing increased by  $2.33 \pm 0.33$  with OST treatment, compared with APP/PS1 mice ( $F$  value = 26.90, # $P < 0.05$ , Fig. 1C). In addition, the time spent in target quadrant also increased in OST group, compared with APP/PS1 mice ( $F$  value = 38.87, ## $P < 0.01$ , Fig. 1D). These results indicated that OST treatment significantly improved the learning and memory function in APP/PS1 mice.

#### 3.2. OST ameliorated the histological changes of brains in APP/PS1 mice

H&E staining was used to observe the histological changes, the results showed that there were a large number of neuronal cells necrosis and injured neurons with an unclear architecture, nucleus pyknosis in APP/PS1 mice. After OST treatment, the damage was ameliorated in hippocampal area (Fig. 2A). Subsequently, the results from Nissl staining embedded that the number of neurons was significantly reduced in the hippocampal area in APP/PS1 group, however, treatment

with OST increased the number of neuronal cells (Fig. 2B). These results indicated that OST could ameliorate the histological changes of brains in APP/PS1 mice.

#### 3.3. OST decreased tau protein phosphorylation and inhibited cells apoptosis in APP/PS1 mice brain

In the present study, we extracted the total protein of brains, in order to investigate the expressions of total tau and phosphorylated tau (Ser202) through Western blot analysis. As shown in Fig. 3A, the level of p-tau was significantly higher in APP/PS1 brain than that not only in the control group, but also in OST treated group. But, the expression of total tau protein had no significant changes in different groups. The statistical analysis of bands was shown in Fig. 3B, the protein expression of p-tau/tau was decreased by  $24.00 \pm 6.80\%$  ( $87.67 \pm 4.70\%$  in APP/PS1 group vs.  $63.67 \pm 4.91\%$  in OST treatment,  $F$  value = 22.45, # $P < 0.05$ ). The results displayed that OST could significantly decrease the phosphorylation of tau protein.

Tau proteins were critical in assembly as well as maintain of the structural integrity of microtubules. A consequence of tau phosphorylation in AD caused to the destruction of microtubule network, and ultimately neural cells apoptosis [27]. Thus, we used TUNEL assay to detect the apoptotic cells in brain sections (Fig. 3C). The percentage of red cells (TUNEL-labeled) out of the total number cells (DAPI-positive) in APP/PS1 mice increased about  $106.00 \pm 8.20\%$  and  $118.30 \pm 13.31\%$  in CA3 and DG area, respectively, compared with control group ( $F$  value = 61.42, \*\* $P < 0.01$ , Fig. 3D;  $F$  value = 48.47, \*\* $P < 0.01$ , Fig. 3E). But, OST significantly decreased the percentage of apoptotic cells, compared with APP/PS1 group ( $63.33 \pm 8.41\%$  vs.  $123.30 \pm 7.86\%$  of CA3 area, ## $P < 0.01$ , Fig. 3D;  $84.67 \pm 6.44\%$  vs.  $134.30 \pm 12.99\%$  of DG area, # $P < 0.05$ , Fig. 3E).

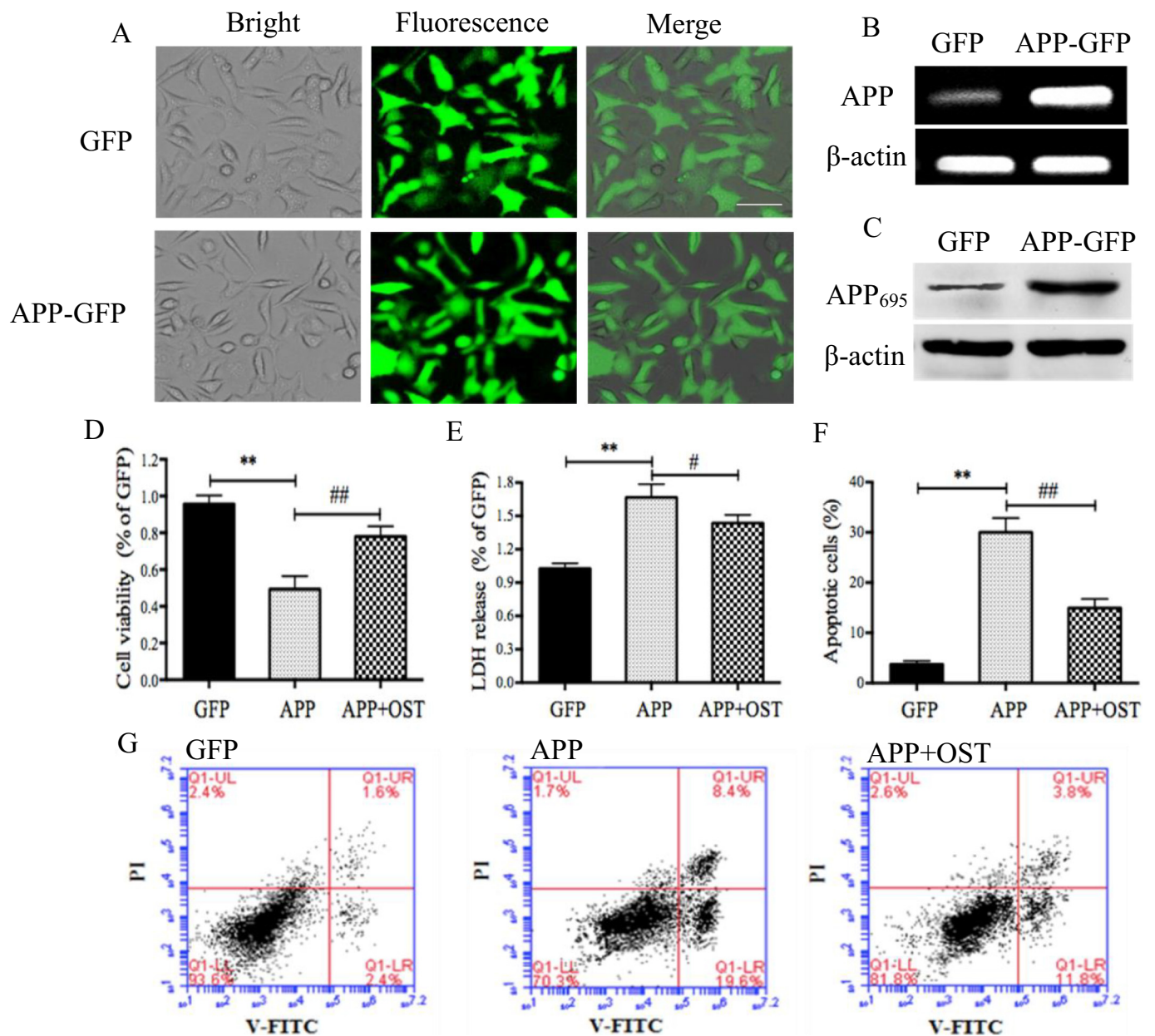


**Fig. 5.** The neuroprotective effects of Osthole on APP-SH-SY5Y cells.

A: Lenti-GFP and Lenti-APP-GFP were transfected into SH-SY5Y cells, respectively. Scale bar = 20  $\mu$ m. B: APP mRNA expression was increased, as determined by RT-PCR. C: APP<sub>695</sub> levels were assessed by Western blot. D: The cell viability was detected by MTT assay. E: The LDH release levels was detected by LDH assay. F: Quantitative analysis of apoptosis in SH-SY5Y cells. G: The percentage of apoptotic cells was measured by flow cytometry. The values are expressed as mean  $\pm$  SD of three independent experiments. (\*\* $P < 0.01$ , \* $P < 0.05$ , # $P < 0.05$ , and ## $P < 0.01$ ,  $n = 3$ , per group).

### 3.4. OST regulated related protein expressions of PI3K/Akt/GSK-3 $\beta$ signaling pathway

According to that GSK-3 $\beta$  played a central role in the pathogenesis of AD and regulated tau phosphorylation, we studied the effect of GSK-3 $\beta$  on AD. GSK-3 $\beta$  was regulated by multiple mechanisms, including PI3K/Akt signaling pathway. We examined that the phosphorylation levels of Akt (Ser473) and GSK-3 $\beta$  (Ser9) to investigate the potential involvement of PI3K/Akt/GSK-3 $\beta$  signaling pathway in the OST-treated neuroprotection against phosphorylated tau (Fig. 4A). As shown in Fig. 4B–D, the levels of PI3K, phosphorylated Akt and GSK-3 $\beta$  was significantly decreased in APP/PS1 group ( $F$  value = 19.20, \* $P < 0.05$ , Fig. 4B;  $F$  value = 19.90, \*\* $P < 0.01$ , Fig. 4C;  $F$  value = 40.45, \*\* $P < 0.01$ , Fig. 4D). However, treatment with OST at dose of 20 mg/kg significantly increased the levels of PI3K, phosphorylated Akt and

GSK-3 $\beta$  protein (# $P < 0.05$ , Fig. 4B; # $P < 0.05$ , Fig. 4C; # $P < 0.05$ , Fig. 4D). Whereas, there had no significant differences between total Akt and GSK-3 $\beta$ , respectively. Therefore, the results showed that OST could up-regulate related the levels of proteins in PI3K/Akt/GSK-3 $\beta$  signaling pathway.

### 3.5. OST had neuroprotective effects in SH-SY5Y cells with transfected APP

To determine the neuroprotective effects of OST in vitro, an AD cells model was established successfully with overexpression of APP. The mutant APP<sub>695</sub> gene and pCDH-CMV-MCS-EF1-copGFP vector (System Biosciences, USA) were transfected into SH-SY5Y cells. Green fluorescence was observed in each group cells using fluorescence microscope in Fig. 5A. Then, the expressions of APP mRNA and protein were significantly increased in APP group, but, there almost little APP

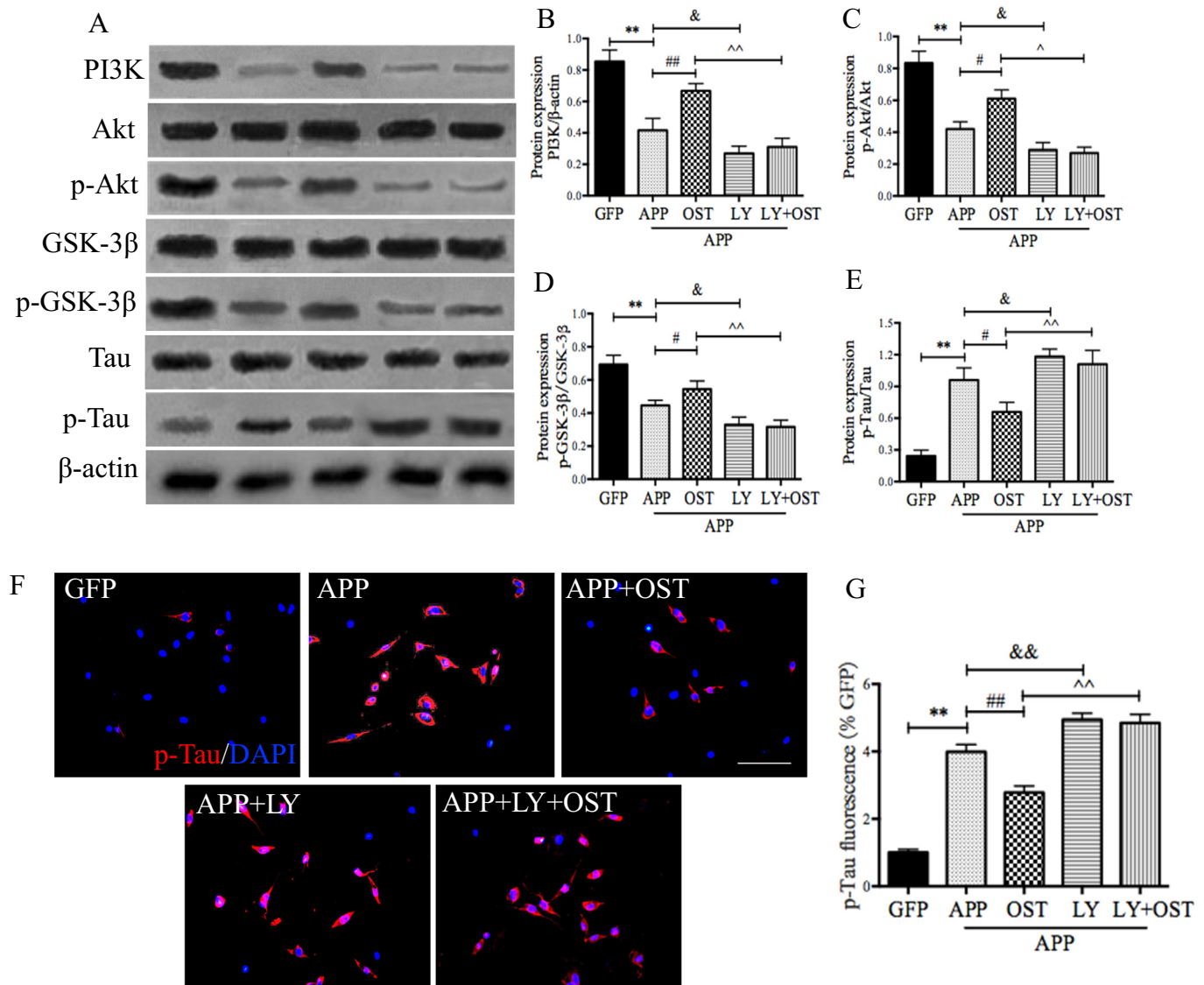


**Fig. 6.** The activate effect of Osthole on PI3K/Akt/GSK-3 $\beta$  signaling pathway. A: The bands of proteins of PI3K/Akt/GSK-3 $\beta$  signaling pathway. B–E: Semi-quantitative analysis of PI3K (B), p-Akt/Akt (C), p-GSK-3 $\beta$ /GSK-3 $\beta$  (D), p-Tau/Tau (E) levels by densitometry. F: The p-Tau protein was detected by immunofluorescent staining. G: Quantitative analysis of fluorescence intensity in APP-SH-SY5Y cells. (\*\* $P < 0.01$ , \* $P < 0.05$ , ## $P < 0.01$ , & $P < 0.05$ , && $P < 0.01$ ,  $\tilde{P} < 0.05$ , and  $\tilde{\tilde{P}} < 0.01$ ,  $n = 3$ , per group).

expression in GFP group (Fig. 5B and C). We concluded that an AD model in SH-SY5Y cells were established successfully with no neurotoxicity.

We further investigated that neuroprotective effects of OST in AD cells using MTT assay and LDH assay. From the result of MTT assay, we found that OST could significantly promote cell viability of AD cells ( $49.33 \pm 4.09$  vs.  $95.67 \pm 2.72\%$  in GFP group,  $F$  value = 47.47, ## $P < 0.01$ , Fig. 5D). From the result of LDH assay, we found that the LDH release decreased with OST treatment, compared AD cells ( $F$  value = 43.59, \* $P < 0.05$ , Fig. 5E). These results indicated that OST had neuroprotective effects in SH-SY5Y cells with overexpression of APP. Moreover, cells apoptosis was measured by Flow cytometry. Different phases of apoptotic cells with both annexin V-FITC positive and PI positive, are represented in the upper and lower right quadrants, which were used to quality the rate of apoptosis. The percentage of apoptotic cells with OST treatment decreased by 15.10%, compared to the APP-SH-SY5Y cells ( $14.93 \pm 1.04$  vs.  $30.03 \pm 1.62\%$ ,  $F$  value = 135.40, ## $P < 0.01$ , Fig. 5F). Based on the results obtained, we concluded that OST exerted effect of protection in APP-SH-SY5Y

cells, also significantly suppressed apoptosis.

### 3.6. OST decreased Tau phosphorylation by activation in PI3K/Akt/GSK-3 $\beta$ signaling pathway

PI3K/Akt/GSK-3 $\beta$  signaling pathway has been suggested to be vital for GSK-3 $\beta$ -mediated the phosphorylation of tau at Ser202 in AD. To determine the role of PI3K on the underlying mechanism that OST attenuated the phosphorylation of tau, we assessed the influence of LY294002, a specific inhibitor of PI3K [28]. As shown in Fig. 6A, total Akt and GSK-3 $\beta$  had no significant difference in each group. Interestingly, the tendency of changes of PI3K, phosphorylated Akt at Ser473 site and GSK-3 $\beta$  at Ser9 site proteins in AD cells model in vitro was similar in APP/PS1 mice in vivo, respectively. However, using PI3K was blocked with LY294002, the expression of PI3K protein was significantly inhibited, in addition, and the expressions of phosphorylated Akt and GSK-3 $\beta$  proteins were decreased in APP-SH-SY5Y cells with or without OST treatment ( $F$  value = 50.10,  $\tilde{P} < 0.01$ , Fig. 6B;  $F$  value = 60.24,  $\tilde{P} < 0.05$ , Fig. 6C;  $F$  value = 36.57,  $\tilde{\tilde{P}} < 0.01$ ,

Fig. 6D), compared with OST alone group, and had no significant differences between two groups (Fig. 6B–D).

A $\beta$ -induced tau protein hyperphosphorylation, an important feature of AD, could cause destabilization of microtubules and apoptosis of the neural cells. It had been shown that hyperphosphorylated tau appears in APP/PS1 mice brain, in this study, we are supposed to detect the expression of phosphorylated tau by Western blot analysis and immunofluorescence assay (Fig. 6A and F). As shown in Fig. 6E and G, the results from bands and immunofluorescence intensity of phosphorylated tau at Ser202 site were significantly higher in APP-SH-SY5Y cells than in OST treated APP-SH-SY5Y cells ( $F$  value = 40.48,  $\tilde{P} < 0.01$ , Fig. 6E;  $F$  value = 211.30,  $\tilde{P} < 0.01$ , Fig. 6G). Meanwhile, the total tau protein did not change much with or without OST treatment. These further results in vitro could indicate that the inhibitory effect of OST on tau phosphorylation depends on the activation in PI3K/Akt/GSK-3 $\beta$  signaling pathway.

#### 4. Discussion

AD was the most prevalent neurodegenerative disorder in aging populations worldwide. Senile plaques (SPs) and intracellular neurofibrillary tangles (NFTs) are two pathological features of AD [29]. Although, as known, A $\beta$  plays a critical role in AD, increasing evidences have indicated that aberrant tau phosphorylation and oligomerization are likely central to the disease process [30,31]. NFTs are consist of abnormal hyperphosphorylated tau protein. In AD brains, tau protein hyperphosphorylation occurred at several Ser or Thr phosphorylated sites, including Ser202, Ser396, Ser404, Thr205, Thr181, etc. These hyperphosphorylated tau proteins will cause to cytoskeletal destabilization, apoptotic cells and eventually memory dysfunction [32]. Obviously, it is an important task to research and develop the drugs with inhibitory effect on tau protein hyperphosphorylation in neural cells exposed to A $\beta$ .

OST, an effective monomer in Chinese medicinal plants, has taken considerable attention due to its diverse pharmaceutical functions. OST has anti-inflammatory [33], anti-apoptosis [34], anti-oxidative stress and neuroprotective properties that makes it promising for therapeutic applications [34]. Our previous study, at the A $\beta$  levels, has displayed that OST could decrease the activation of BACE1 via up-regulation of miR-107. But, with regard to the inhibitory effect of OST on tau protein phosphorylation and its underlying mechanism were unknown. Thus, in present study, we aimed to further investigate the neuroprotective effects of OST against tau protein phosphorylation not only in APP/PS1 mice at 6th month but also in APP<sub>swe</sub> transfected SH-SY5Y cells, which can be behalf of the pathological characteristics of AD. Firstly, the result from Morris water maze was determined that OST could significantly improve the learning and memory deficits. After the test trail, the brains were collected and then cut into sections (7  $\mu$ m), which were used to H & E and Nissl staining. Compared with APP/PS1 mice, there was less neuronal damage in the CA3 and DG of the hippocampus of OST treated mice (Fig. 2A–B). Importantly, tau protein phosphorylation level was significantly decreased with OST treated. As known, abnormally phosphorylated tau will cause itself to lose biological activity, become toxic, which led to cell apoptosis. Therefore, the percentage of apoptotic cells in brain sections and APP-SH-SY5Y cells was further detected by TUNEL assay and Flow cytometry, respectively. As expected, compared to APP/PS1 group, the percentage of cells apoptosis was decreased by 60.00  $\pm$  11.51% in CA3 and 49.67  $\pm$  14.50% in DG area with OST treatment (Fig. 3D–E). In addition, OST also reduced the percentage of apoptotic SH-SY5Y cells with APP transfected (Fig. 5F). These results showed that the regulation effect of OST on protective cells apoptosis may be effective to tau protein hyperphosphorylation stimulation.

Various kinases and phosphatases are involved in the regulation of tau phosphorylation. Of those, GSK-3 $\beta$ , which a critical tau kinase, was a downstream target of PI3K/Akt signaling pathway [35]. A large

number of evidence displayed that the PI3K/Akt pathway was down-regulated in AD patients, if PI3K/Akt was activated, it would significantly reduce tau-induced neurotoxicity [36]. Therefore, we at first investigated the related proteins levels in APP/PS1 mice, our data showed that OST could increase PI3K, phosphorylated Akt, and GSK-3 $\beta$  protein levels, compared with APP/PS1 group (Fig. 4B–D). To further explore the underlying mechanism, co-treatment of PI3K pathway inhibitor LY294002 with OST abolished the activation effect of OST on PI3K pathway, as well as the phosphorylation potential at Ser202 site of GSK-3 $\beta$ . When the pathway was blocked, there had no significant differences between LY294002 alone and LY294002 with OST co-treatment, it revealed that the effect of OST on PI3K pathway was inhibited by LY294002. Here, it was worthy pointing out that we found that the neuroprotective effect of OST on tau hyperphosphorylation was directly related to the regulation of PI3K/Akt-dependent GSK-3 $\beta$  signaling pathway.

Taken together, the present study indicated that OST ameliorated learning and memory impairment in behavioral tasks in mice. Moreover, we provide the demonstration that OST exerted neuroprotective effects against the phosphorylated tau protein levels via the activation of PI3K signaling pathway. Thus, these data demonstrated that OST may represent a promising therapeutic strategy to attenuate AD and other tau pathology-related neuronal degenerative diseases.

#### Acknowledgments

This project was funded by the National Natural Science Foundation of China (No. 81173580).

#### Conflict of interest

The authors declare no conflict of interest.

#### References

- [1] M.A. Lopez-Toledano, M. Ali Faghihi, N.S. Patel, C. Wahlestedt, Adult neurogenesis: a potential tool for early diagnosis in Alzheimer's disease, *J. Alzheimers Dis.* 20 (2) (2010) 395–408.
- [2] Y. Du, Y. Zhao, C. Li, Q. Zheng, J. Tian, Z. Li, T.Y. Huang, W. Zhang, H. Xu, Inhibition of PKC $\delta$  reduces amyloid- $\beta$  levels and reverses Alzheimer disease phenotypes, *J. Exp. Med.* 215 (6) (2018) 1665–1677 Jun 4.
- [3] P.H. Reddy, Abnormal tau, mitochondrial dysfunction, impaired axonal transport of mitochondria, and synaptic deprivation in Alzheimer's disease, *Brain Res.* 1415 (2011) 136–148 Sep 30.
- [4] A.L. Woerman, A. Aoyagi, S. Patel, S.A. Kazmi, I. Lobach, L.T. Grinberg, A.C. McKee, W.W. Seeley, S.H. Olson, S.B. Prusiner, Tau prions from Alzheimer's disease and chronic traumatic encephalopathy patients propagate in cultured cells, *Proc. Natl. Acad. Sci. U. S. A.* 113 (50) (2016) E8187–E8196 Dec 13.
- [5] J.T. Pedersen, E.M. Sigurdsson, Tau immunotherapy for Alzheimer's disease, *Trends Mol. Med.* 21 (6) (2015) 394–402 Jun.
- [6] G.S. Bloom, Amyloid- $\beta$  and tau: the trigger and bullet in Alzheimer disease pathogenesis, *JAMA Neurol.* 71 (4) (2014) 505–508. Apr.
- [7] S. Matsuda, Y. Nakagawa, A. Tsuji, Y. Kitagishi, A. Nakanishi, T. Murai, Implications of PI3K/AKT/PTEN signaling on superoxide dismutases expression and in the pathogenesis of Alzheimer's disease, *Diseases* 6 (2) (2018) Apr 20.
- [8] W. Huang, P. Cheng, K. Yu, Y. Han, M. Song, Y. Li, Hyperforin attenuates aluminum-induced A $\beta$  production and Tau phosphorylation via regulating Akt/GSK-3 $\beta$  signaling pathway in PC12 cells, *Biomed. Pharmacother.* 96 (2017) 1–6 Dec.
- [9] J. Avila, F. Wandosell, F. Hernández, Role of glycogen synthase kinase-3 in Alzheimer's disease pathogenesis and glycogen synthase kinase-3 inhibitors, *Expert. Rev. Neurother.* 10 (5) (2010) 703–710 May.
- [10] H. Zhang, X. Yang, X. Qin, Q. Niu, Caspase-3 is involved in aluminum-induced impairment of long-term potentiation in rats through the akt/GSK-3 $\beta$  pathway, *Neurotox. Res.* 29 (4) (2016) 484–494 May.
- [11] G. Jiang, J. Liu, B. Ren, Y. Tang, L. Owusu, M. Li, J. Zhang, L. Liu, W. Li, Anti-tumor effects of osthole on ovarian cancer cells in vitro, *J. Ethnopharmacol.* 193 (2016) 368–376 Dec 4.
- [12] T. Okamoto, T. Kawasaki, O. Hino, Osthole prevents anti-Fas antibody-induced hepatitis in mice by affecting the caspase-3-mediated apoptotic pathway, *Biochem. Pharmacol.* 65 (4) (2003) 677–681 Feb 15.
- [13] X.L. Wang, X. Shang, Y. Cui, X. Zhao, Y. Zhang, M.L. Xie, Osthole inhibits inflammatory cytokine release through PPAR $\alpha$ / $\gamma$ -mediated mechanisms in LPS-stimulated 3T3-L1 adipocytes, *Immunopharmacol. Immunotoxicol.* 37 (2) (2015) 185–192. Apr.
- [14] S. Li, Y. Yan, Y. Jiao, Z. Gao, Y. Xia, L. Kong, Y. Yao, Z. Tao, J. Song, Y. Yan,

- G. Zhang, J. Yang, Neuroprotective effect of osthole on neuron synapses in an Alzheimer's disease cell model via upregulation of MicroRNA-9, *J. Mol. Neurosci.* 60 (1) (2016) 71–81 2016 Sep.
- [15] Y.H. Yan, S.H. Li, H.Y. Li, Y. Lin, J.X. Yang, Osthole protects bone marrow-derived neural stem cells from oxidative damage through PI3K/Akt-1 pathway, *Neurochem. Res.* 42 (2) (2017) 398–405 Feb.
- [16] Y. Yan, L. Kong, Y. Xia, W. Liang, L. Wang, J. Song, Y. Yao, Y. Lin, J. Yang, Osthole promotes endogenous neural stem cell proliferation and improved neurological function through Notch signaling pathway in mice acute mechanical brain injury, *Brain Behav. Immun.* 67 (2018) 118–129 Jan.
- [17] Y. Jiao, L. Kong, Y. Yao, S. Li, Z. Tao, Y. Yan, J. Yang, Osthole decreases beta amyloid levels through up-regulation of miR-107 in Alzheimer's disease, *Neuropharmacology* 108 (2016) 332–344 Sep.
- [18] Y. Yao, Z. Gao, W. Liang, L. Kong, Y. Jiao, S. Li, Z. Tao, Y. Yan, J. Yang, Osthole promotes neuronal differentiation and inhibits apoptosis via Wnt/ $\beta$ -catenin signaling in an Alzheimer's disease model, *Toxicol. Appl. Pharmacol.* 289 (3) (2015) 474–481 Dec 15.
- [19] H. Choi, H.H. Park, K.Y. Lee, N.Y. Choi, H.J. Yu, Y.J. Lee, J. Park, Y.M. Huh, S.H. Lee, S.H. Koh, Coenzyme Q10 restores amyloid beta-inhibited proliferation of neural stem cells by activating the PI3K pathway, *Stem Cells Dev.* 22 (15) (2013) 2112–2120. Aug 1.
- [20] E.M. Toledo, N.C. Inestrosa, Activation of Wnt signaling by lithium and rosiglitazone reduced spatial memory impairment and neurodegeneration in brains of an APP<sup>sw</sup>/PSEN1<sup>D9</sup> mouse model of Alzheimer's disease, *Mol. Psychiatry* 15 (3) (2010) 272–285 Mar. (228).
- [21] S.H. Li, P. Gao, L.T. Wang, Y.H. Yan, Y. Xia, J. Song, H.Y. Li, J.X. Yang, Osthole stimulated neural stem cells differentiation into neurons in an Alzheimer's disease cell model via upregulation of MicroRNA-9 and rescued the functional impairment of hippocampal neurons in APP/PS1 transgenic mice, *Front. Neurosci.* 11 (2017) 340 Jun 13.
- [22] G. Gontier, C. George, Z. Chaker, M. Holzenberger, S. Aïd, Blocking IGF signaling in adult neurons alleviates Alzheimer's disease pathology through amyloid- $\beta$  clearance, *J. Neurosci.* 35 (33) (2015) 11500–11513. Aug 19.
- [23] Y. Xia, L. Kong, Y. Yao, Y. Jiao, J. Song, Z. Tao, Z. You, J. Yang, Osthole confers neuroprotection against cortical stab wound injury and attenuates secondary brain injury, *J. Neuroinflammation* 12 (2015) 155 Sep 4.
- [24] J. Yang, Y. Yan, Y. Xia, T. Kang, X. Li, B. Ciric, H. Xu, A. Rostami, G.X. Zhang, Neurotrophin 3 transduction augments remyelinating and immunomodulatory capacity of neural stem cells, *Mol. Ther.* 22 (2) (2014) 440–450 Feb.
- [25] X. Chen, J. Zhang, Y. Fang, C. Zhao, Y. Zhu, Ginsenoside Rg1 delays tert-butyl hydroperoxide-induced premature senescence in human WI-38 diploid fibroblast cells, *J. Gerontol. A Biol. Sci. Med. Sci.* 63 (3) (2008) 253–264 Mar.
- [26] I.S. Lee, K. Jung, I.S. Kim, K.I. Park, Amyloid- $\beta$  oligomers regulate the properties of human neural stem cells through GSK-3 $\beta$  signaling, *Exp. Mol. Med.* 45 (2013) e60, <https://doi.org/10.1038/emmm.2013.125> Nov 15.
- [27] Y. Kitagishi, A. Nakanishi, Y. Ogura, S. Matsuda, Dietary regulation of PI3K/AKT/GSK-3 $\beta$  pathway in Alzheimer's disease, *Alzheimers Res. Ther.* 6 (3) (2014) 35 Jun 20.
- [28] S.I. Gharbi, M.J. Zvelebil, S.J. Shuttleworth, T. Hancox, N. Saghir, J.F. Timms, M.D. Waterfield, Exploring the specificity of the PI3K family inhibitor LY294002, *Biochem. J.* 404 (1) (2007) 15–21 May 15.
- [29] P. Rudrabhatla, H. Jaffe, H.C. Pant, Direct evidence of phosphorylated neuronal intermediate filament proteins in neurofibrillary tangles (NFTs): phosphoproteomics of Alzheimer's NFTs, *FASEB J.* 25 (11) (2011) 3896–3905 Nov.
- [30] M. Goedert, NEURODEGENERATION. Alzheimer's and Parkinson's diseases: The prion concept in relation to assembled A $\beta$ , tau, and  $\alpha$ -synuclein, *Science* 349 (6248) (2015) 1255555. Aug 7.
- [31] M.M. Mielke, N.J. Haughey, V.V.R. Bandaru, H. Zetterberg, K. Blennow, U. Andreasson, S.C. Johnson, C.E. Gleason, H.M. Blazel, L. Puglielli, M.A. Sager, S. Asthana, C.M. Carlsson, Cerebrospinal fluid sphingolipids,  $\beta$ -amyloid, and tau in adults at risk for Alzheimer's disease, *Neurobiol. Aging* 35 (11) (2014) 2486–2494 Nov.
- [32] F.M. LaFerla, S. Oddo, Alzheimer's disease: Abeta, tau and synaptic dysfunction, *Trends Mol. Med.* 11 (4) (2005) 170–176. Apr.
- [33] X. Zhao, F. Wang, R. Zhou, Z. Zhu, M. Xie, PPAR $\alpha$ / $\gamma$  antagonists reverse the ameliorative effects of osthole on hepatic lipid metabolism and inflammatory response in steatohepatic rats, *Inflammopharmacology* 26 (2) (2018) 425–433. Apr.
- [34] Y. Shokoohinia, L. Hosseinzadeh, M. Moieni-Arya, A. Mostafaie, H.R. Mohammadi-Motlagh, Osthole attenuates doxorubicin-induced apoptosis in PC12 cells through inhibition of mitochondrial dysfunction and ROS production, *Biomed. Res. Int.* 2014 (2014) 156848.
- [35] M. Medina, J. Avila, Understanding the relationship between GSK-3 and Alzheimer's disease: a focus on how GSK-3 can modulate synaptic plasticity processes, *Expert. Rev. Neurother.* 13 (5) (2013) 495–503 May.
- [36] H. Lou, P. Fan, R.G. Perez, H. Lou, Neuroprotective effects of linarin through activation of the PI3K/Akt pathway in amyloid- $\beta$ -induced neuronal cell death, *Bioorg. Med. Chem.* 19 (13) (2011) 4021–4027 Jul 1.